Friction stir welding of ABS-15Al sheets by introducing compatible semi-consumable shoulder-less pin of PA6-50Al

Ranvijay Kumar, Rupinder Singh, IPS Ahuja

PII: S0263-2241(18)30834-0
DOI: https://doi.org/10.1016/j.measurement.2018.09.005
Reference: MEASUR 5863

To appear in: *Measurement*

Received Date: 13 March 2018
Revised Date: 29 July 2018
Accepted Date: 2 September 2018

Please cite this article as: R. Kumar, R. Singh, I. Ahuja, Friction stir welding of ABS-15Al sheets by introducing compatible semi-consumable shoulder-less pin of PA6-50Al, *Measurement* (2018), doi: https://doi.org/10.1016/j.measurement.2018.09.005

Friction stir welding of ABS-15Al sheets by introducing compatible semi-consumable shoulder-less pin of PA6-50Al

[1,2]Ranvijay Kumar [1]Rupinder Singh*, [2]IPS Ahuja
[1]Dept. of Production Engineering, Guru Nanak Dev Engineering College, Ludhiana (India)
[2]Dept. of Mech. Engineering, Punjabi University, Patiala (India)
[1,2]ranvijayk12@gmail.com [1]rupindersingh78@yahoo.com, ,[2]ahujaips@gmail.com
*Corresponding author

Abstract

This study demonstrates the solution for compatibility issues between two dissimilar thermoplastic materials for friction stir welding (FSW) applications. The joints of similar thermoplastic materials possesses good mechanical strength and uniform morphological characteristics but dissimilar thermoplastic are difficult to join as they are having large variation in molecular weight, carbon chain length, melt flow index (MFI) and melting point etc. In the present study, MFI of dissimilar thermoplastics namely: acrylonitrile butadiene styrene (ABS) and polyamide (PA)6 was modeled by reinforcement of Al metal powder for enhancing the material compatibility. Reinforcement of 15% Al metal powder (by weight) to ABS (as ABS-15Al) and 50% to PA6 (as PA-50Al) resulted in the similar MFI range of 11.57g/10min and 11.97g/10 (with similar melting point range) confirmed the enhanced material compatibility with possibilities of sound FSW joints. Twin screw extrusion (TSE) and fused deposition modeling (FDM) were used to prepare the specimens of ABS-15Al and PA6-50Al and FSW was performed on conventional vertical milling setup. Further multi response optimization has been performed for establishing best settings of input process parameters.

Keywords: Friction stir welding, melt flow index, thermal properties, thermoplastics

1. Introduction

Dissimilar thermoplastics are having different mechanical, thermal, rheological, chemical and morphological characterises, which hinders its joining application; especially when thermoplastic needs to be compatible in basic nature e.g. in solid state welding [1]. ABS and PA6 are two dissimilarly characterized polymers which can be differentiated by their MFI [2].The MFI of thermoplastic material can be modified by reinforcement of micro-sized metal powder to polymer's matrix [3]. FSW as solid state welding technique is best applicable for similar material since similar materials possesses better joining compatibility [4]. Polymer compatibility is an important issue for its application in different engineering areas. It has been reported that pores and permeability of the polymeric blend is dependent upon rheological properties of polymers [5]. Sometimes blended materials result in poor mechanical strength [6]. The issue of non-compatibility occurs because thermoplastics are categorized by their unique

carbon chain length, flow ability, morphology, molecular weight, molecular density, thermal behaviour and chemical behaviour [7, 8]. It was demonstrated that incorporation of glass fibre to polyethylene terephthalate (PET) provided better impact strength [9]. Similarly, hydroxyl terminated poly-dimethyl siloxane introduced to epoxy resin matrix resulted in improved electric properties with minor losses of mechanical properties [10]. Reinforcement of metallic and non-metallic fillers leads to the modification in the mechanical [12] and morphological [13] characteristics of the polymer matrix as well as polymer compatibility for joining and mixing. Mono-disperse silica particle in blend of polyethylene oxide and poly-isobutylene has resulted into massive rheological changes [14]. Similarly sisal fibre introduced in the ploy-lactic acid (PLA) matrix by the extrusion-injection moulding resulted in improved tensile and flexural modulus [14].

FSW is a conventional solid-state joining process that uses a non-consumable tool to join two facing work-pieces without melting the work-piece material. A pin is fixed with shoulder is inserted to the material by rotation provides friction generation between surface of work-piece and tool material. The basic aim of shoulder is to control the material flow as an outcome of friction between work-piece and pin. Fig. 1 shows schematic of FSW process.

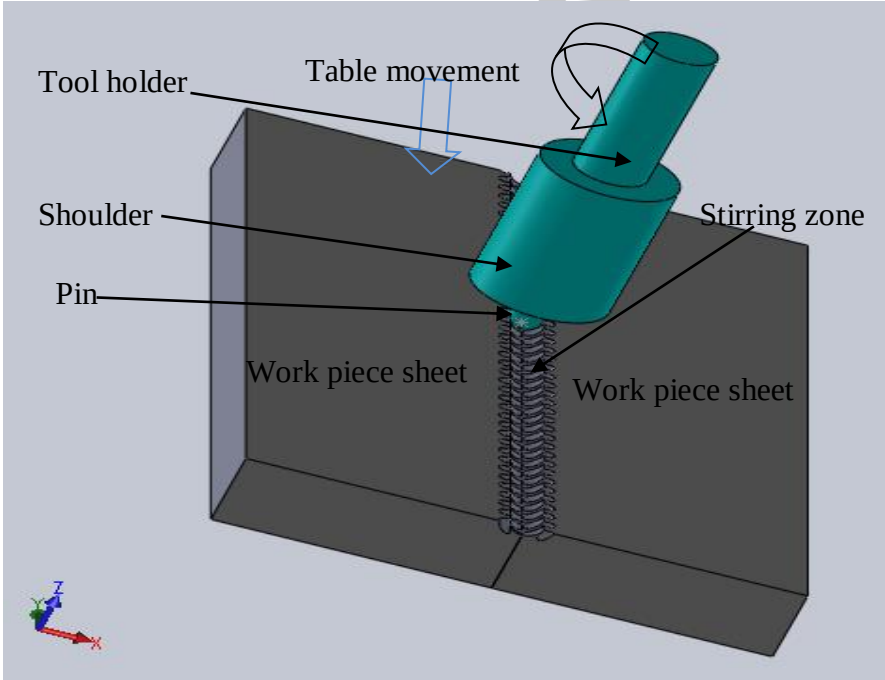

Fig. 1 Basic configuration of FSW process for thermoplastic joining

The heat generation during the FSW process is the measure of the welding strength which is largely dependent upon the material compatibility, rotational speed, workpiece and tool dimensions, material of shoulder and pin, tool rotation angle, transverse speed etc. It has been reported that for 50×30×4 mm sheet of high density polyethylene (HDPE) the FWS is eligible to weld at tool rotational speed of 1500, 2100, 3000rpm , tool transverse speed at 45, 75, 115mm/min and at tilt angle of 1º, 2º, 3º. This study outlines that tool rotation speed contributed

maximum for joint strength (around 73.85%) [15]. Squeo et al. have conducted similar operations for 150×60×6mm sheet of (medium density polyethylene) MDPE at the rotational speed between 1400-2000rpm, tilt angle 1-2^{o} and travel speed of 15mm/min [16]. This study highlights that rational speed contributes maximum for the change in the elongation as well as tilt angle contributes maximum for the change in the tensile strength of the MDPE joints produced by FSW [17]. Another study has been reported for poly methyl methacrylate (PMMA) specimen having sample size of 100×25×3mm. It was observed that PMMA sample requires 500-200rpm, 5.5-12sec welding time, joining pressure of 3 bar and plunge depth of 3.5-4mm [18,19].

Friction-based injection clinching joining technique (F-ICJ) for production of hybrid structure of polyetherimide (PEI-AA6082-T6) requires ultra high rotational speed in between 7500-20000rpm, frictional force of 0.2-0.MPa and frictional time of 2500-5000milliseconds [20]. Some studies have reported that for production of 2mm thick weld of carbon reinforced polyamide (PA66) laminates by the friction spot welding, it requires 1000-3000rpm, 1.8-2.2 plunge depth and 3.6-7.5sec frictional time [21]. FSW for 10mm PMMA plates requires 700rpm rotational speed, advancing speed of 25mm/min, 15-35mm shoulder diameter and 5-6mm pin diameter [19]. For sample of 100×100×3 mm with curve thickness of 2.7mm aluminum reinforced polypropylene (AA6082-PP) sheets requires the rotational speed of 1000rpm, feed rate of 100mm/min, 2° tilt angle, 3000N force and 3-7mm pin diameter [22]. Further it has been reported that for joining of polycarbonate (PC)-PC sheets of 90×20×3mm through FSW, tool plunge rate between 8-46mm/min, tool rotation of 1500-5400rpm, pre-heating time of 0-20sec, dwell time 0-20sec and waiting time of 0-20sec the joining is required [23].

It should be noted that welding joints are highly characterized by their micro-structure; mechanical properties and sustainability of welded joints are investigated by thermal, mechanical, tribological and morphological properties [24-28]. Welding of Al to Polyvinyl chloride (PVC) possesses good shear strength sustainability of 16.1MPa which is almost 75% to the parent PVC [29]. Mechanical sustainability of the joints is highly dominated by the role of tool geometry and configuration. As FSW conducted for PP and polyethylene (PE), the optimum pin geometry resulted in the tensile strength 98% to the PE as well as elongation and hardness greater than the base material [25]. HDPE with dimension of 100×200×10 possessed 96% flexural strength as compared to base material at optimum processing conditions (RPM: 1400, transverse speed 25mm/min and shoulder temperature of 100 degree centigrade) [30]. Joints produced by FSW are post processed with technologies like; cleaning, edge removal, heat treatment, joint cutting etc. Abrasive water jet (AJM) is a non-conventional cutting technique which can be used for FSW joint cutting with superior control over surface roughness and dimensional accuracy with no heat affected zone [31-33].

As observed from the reported literature, most of the studies have been conducted for welding/ joining of the similar thermoplastic materials, but very less have been reported for FSW of dissimilar thermoplastic material. Some studies have reported use of the metallic and non-metallic fillers and their processing techniques for uniform blending in thermoplastics. But

hitherto wide gap has been observed in joining of functional prototypes of dissimilar thermoplastics (with compatibility issues) especially in structural engineering applications [1-4, 20, 25, 29].

The present study is focused to solve the material compatibility issues that hinder the joining of the two dissimilar polymers by FSW process with shoulder-less semi consumable pin profile of required dimension. The MFI of the two dissimilar thermoplastics (ABS and PA6) was made compatible by reinforcement of the Al metal powder that offered the better mixing during FSW. Multifactor optimization has been performed to select the best set of process parameters.

2. Experimentation

Initially two sheets of ABS with dimension 50mm×30mm×4mm and cylindrical pin of PA6 with 80mm length and 7-9mm diameter have been prepared on commercial FDM setup. The prepared sheets of ABS were processed at milling setup for FSW by stirring through pin profile (7-9mm diameter) of PA6 at 1000-1200rpm and 30-50 mm/min table speed. The welding process was almost failed and joints were not formed due to uncontrolled material flow during the process. Here it was experienced that ABS and PA6 are the two different materials which have large difference in their melt flow index, carbon chain length, melting point, chemical properties, crystalline vs. amorphous, elongation and tensile characteristics. So the large difference in the mechanical, thermal, morphological, rheological and chemical properties of ABS and PA6 hiders the formation of joints made by FSW. Based upon these observations, systematic experimental procedure has been used to join the ABS sheets with stirring PA6 pin (see Fig. 2).

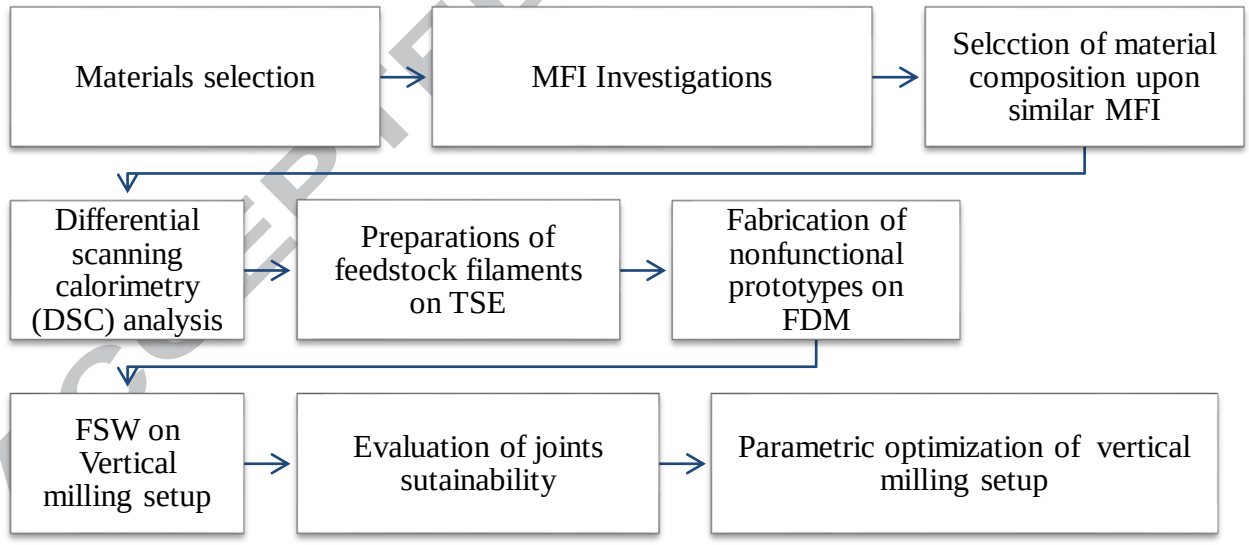

Fig. 2 Experimental procedure to produce welding joints of dissimilar plastic based materials

2.1 Materials and Methods

In this study ABS and PA6 have been selected for final experimentation. The TSE of virgin ABS and PA6 material have been performed for preparations of feedstock filaments (diameter =

1.75±0.05mm). The feedstock filaments of virgin ABS and PA6 were analyzed from mechanical, rheological and thermal view point to understand their basic characteristics. The mechanical properties were evaluated by universal tensile tester (ASTM D628), Melt flow indexer (ASTM D1238) was used to evaluate the MFI and DSC setup was used to evaluate the melting point. It should be noted that material properties of ABS and PA6 were evaluated in 3 consecutive repetitions and average of all have been presented in Table 1.

Table 1

Materials property of virgin ABS and PA6

Material	Peak Load(Kgf)	Peak Strength(MPa)	Shore D Hardness	Melt Flow Index(g/10min)	Melting Point (°C)
ABS	59.2 (Δd = 0.2)	23.40 (Δd = 0.85)	73.0 (Δd = 1.3)	8.76 (Δd = 0.23)	201.22 (Δd = 1.5)
PA6	203.0 (Δd = 0.25)	94.90 (Δd = 1.2)	71.5 (Δd = 1.1)	23.27 (Δd = 0.31)	219.35 (Δd = 1.4)

Where Δd is deviation/ scatter observed while 03 consecutive repetitions

Aluminum metal powder of 300 mesh size (Approx. 50µm grain size) was selected for the reinforcement. The Al metal powder was added in the ABS and PA6 polymer matrix to modify the MFI. For the final FSW operation the steps are presented in Fig. 3. The gap of 0.5mm was maintained between the two work pieces of ABS and then by keeping the pin of PA6 at 1000-1400rpm (with 2mm depth to sheet and 30-50mm table movement) good joint was observed. The gap of 0.5mm was given to support the inward material flow in between the sheets to strengthen the joints.

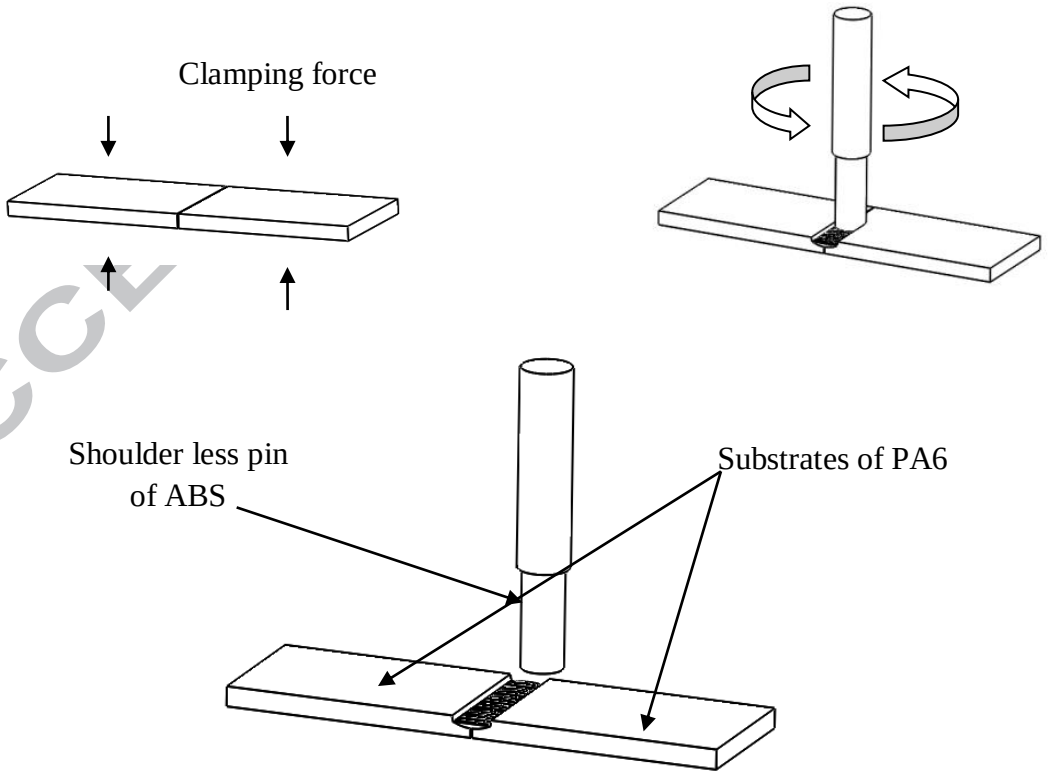

Fig. 3 Steps in friction stir welding though semi consumable pin

2.2 MFI investigations and proportion consideration

It has been observed that in case of ABS polymer matrix by increasing the Al metal filler up to 20%, lead to increase in the MFI, but above this level there was significant decrease in MFI (see Fig. 2). For PA6 polymer matrix, the increase was observed in MFI up to 30% of Al filler but after that increase in the Al fillers, decreased the MFI. From the MFI characterization of ABS and PA6 reinforced with Al metal powder, it should be noted that ABS with 15% Al (MFI= 11.57g/10min) and PA6 with 50% Al (MFI= 11.97g/10min) resulted in the very closer range of MFI. So, for the DSC analysis these two compositions (ABS-15Al and PA6-50Al) have been selected.

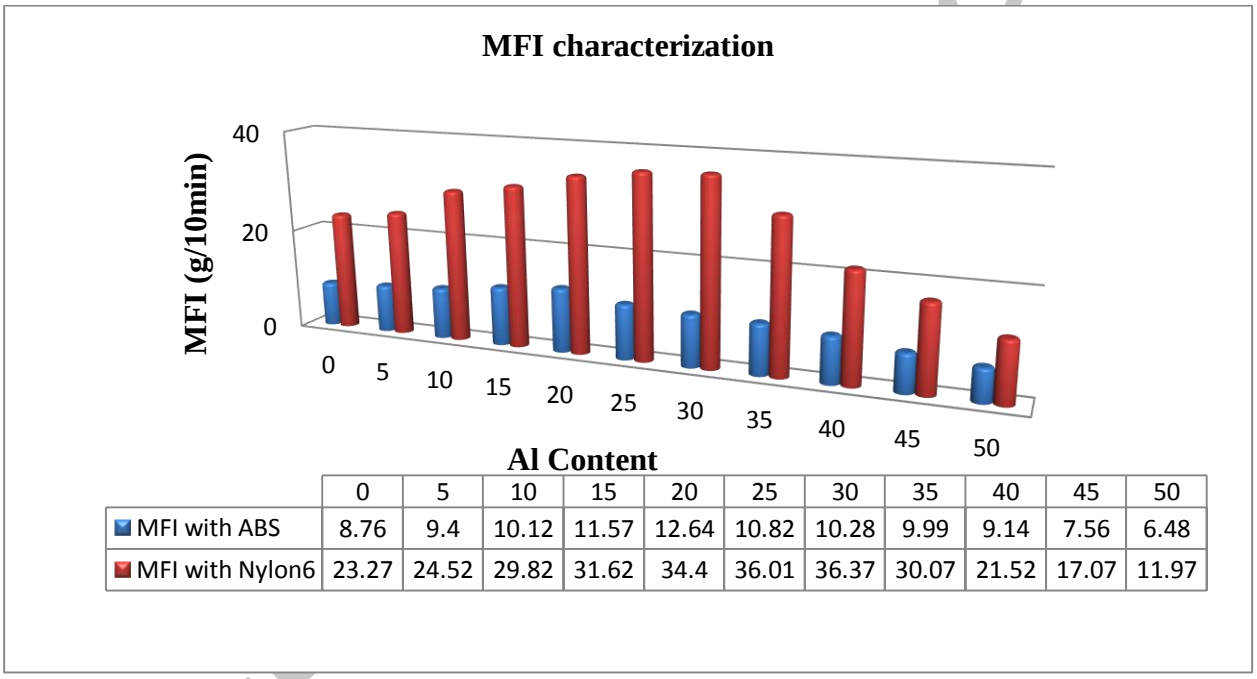

	0	5	10	15	20	25	30	35	40	45	50
MFI with ABS	8.76	9.4	10.12	11.57	12.64	10.82	10.28	9.99	9.14	7.56	6.48
MFI with Nylon6	23.27	24.52	29.82	31.62	34.4	36.01	36.37	30.07	21.52	17.07	11.97

Fig. 4 Variations in MFI of ABS and PA6 over Al proportions

2.3 DSC Analysis

The DSC evaluation was performed under controlled experimental environment conditions of continuous heating (endothermic changes, 10°C/min) and continuous cooling (exothermic changes, 10°C/min) in 30-250°C temperature range through two consecutive cycles at 50ml/min of N_2 gas supply. Under the N_2 gas supply of 50ml/min. DSC curves are plotted (as shown in Fig. 5) under 2 cycle of heating. .For the peak melting of ABS and PA6 there was a large gap of melting point found, but melting point of ABS-15Al and PA6-50Al was obtained considerably similar as 218.11°C and 218.27°C respectively. So it justified the hypotheses that definite proportions of Al content leading to similar MFI also contributed to their similarities in the melting range.

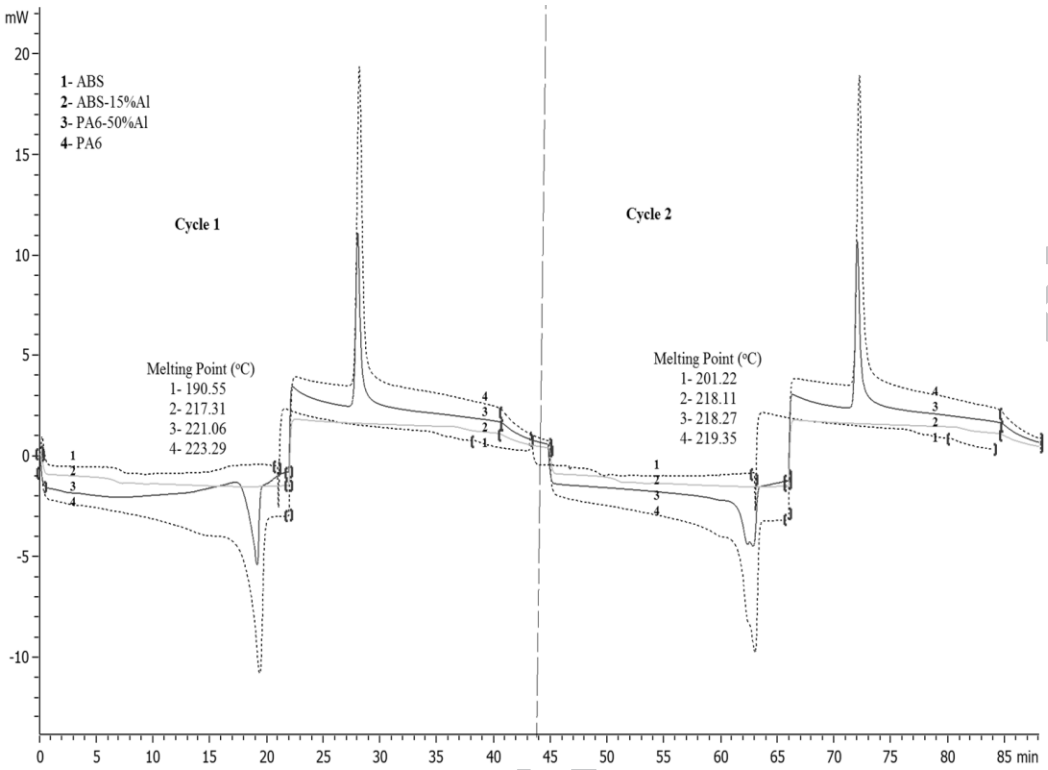

Fig. 5 DSC plots for virgin ABS[1], ABS-15Al[2], PA6-50Al[3] and virgin PA6[4]

2.3 Feedstock filament preparations

TSE is one of the most advanced techniques for the preparations of the feedstock filament and for uniform mixing of the reinforcement agent with polymer matrix. The main advantages of twin-screw extruders (intermeshing co-rotating) are their exceptional mixing capability that gives the remarkable characteristics to extruded products. So, in the present study an intermeshing co-rotating type of TSE has been selected for experimentations (See Fig. 6).

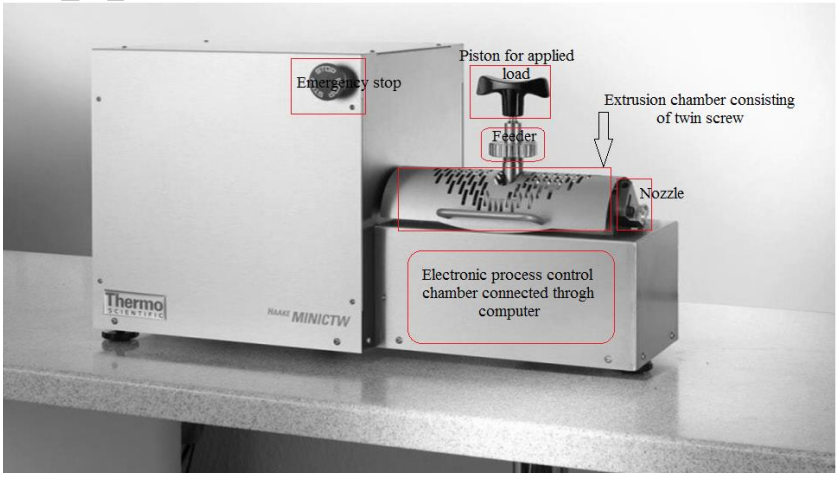

Fig. 6 Photographic view of the experimental setup for extrusion of feedstock filaments and prepared spool of feedstock filament

The TSE is operating between the temperature range of 25-400ºC, rotational speed range of 0-300rpm and torque range of 0-2N.m. The nozzle can be changed from 0.25mm to 2.0mm in diameter as required of applications the pilot experimentation was conducted and input process parameter was decided based upon the uniformity of the filament extruded. Except temperature, nozzle diameter and operating torque were the two other machining parameters which have significant effect on the change in the properties of the obtained feedstock filaments. The temperature for extrusion has been selected as the DSC results obtained (218.11ºC for ABS-15Al and 218.27ºC for PA6-50Al), for better mixing of the Al with ABS and PA6 matrix, the extrusion temperature should be greater than the melting point so the temperature of 220ºC for ABS-15Al and 245ºC for PA6-50Al) has been selected. The acceptable diameter for feedstock filaments to be compatible with FDM is 1.5mm, so the nozzle diameter has been selected as 1.5mm. The screw speed and applied load have been selected based upon the pilot experimentation conducted. Based upon the uniformity achieved the following set of parametric combinations have been selected for ABS-15Al and PA6-50Al; as given in Table 2.

Table 2
Processing setup for preparation of feedstock filaments of ABS-15Al and PA6-50Al

Materials	Temperature (ºC)	Screw speed (RPM)	Applied load (Kg)
ABS-15Al	220	30	20
PA6-50Al	245	20	15

Based upon the processing conditions given in Table 2, the feedstock filaments of ABS-15Al and PA6-50Al have been prepared as shown in Fig. 7.

Fig. 7 Spools of feedstock filaments of ABS-15Al and PA6-50Al

2.4 FDM (Part Fabrication)

Prepared feedstock filaments of ABS-15Al and PA6-50Al were fed to commercial FDM set to fabricate non-functional prototypes for friction welding applications. Fig. 8 shows the pictorial view of commercial FDM setup and parts fabricated in the form of pin and rectangular sheets.

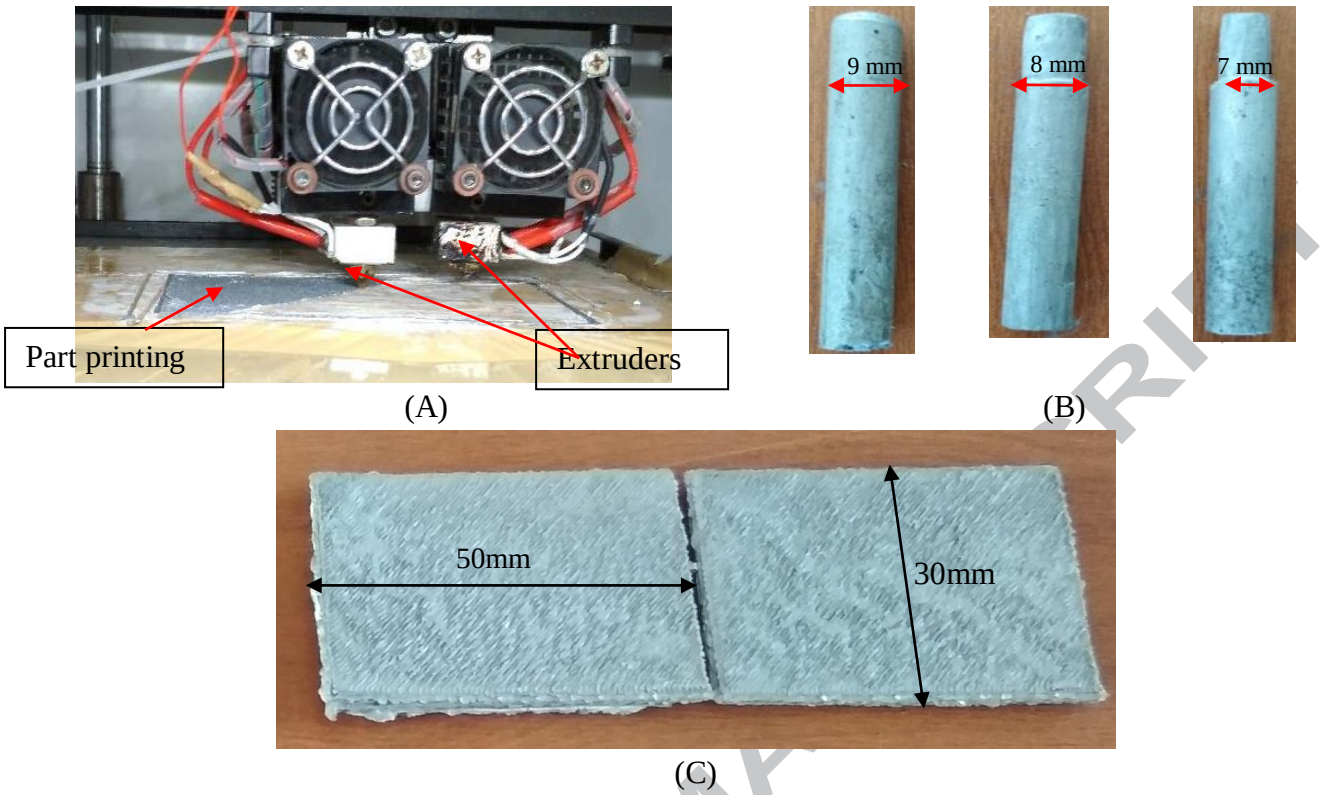

Fig. 8 Photographic view of (A) Part fabrication on FDM, (B) Printed Shoulder less pin of PA6-50Al for FSW and (C) Printed sheets of ABS-15Al for joining

The open source FDM setup has been used under controlled conditions for preparation of functional prototypes with infill density of 0.8, 6 number of perimeter, deposition angle of 60°, nozzle diameter of 0.3mm, filament diameter of 1.75mm, rectilinear fill pattern, perimeter speed of 30mm/s, infill speed of 60mm/s, travel speed of 130mm/s, extruder temperature of 250°C and bed temperature of 55°C. Rectangular sheet was prepared with ABS-15Al whereas PA6-50Al was used to fabricate the pin profile under these same processing conditions (see Fig.8).

2.5 Design of experiment

For joining/welding of prepared sheets, rotational speed, transverse speed, and pin diameter was varied accordingly. Pilot experimentation was performed from 500-2000 RPM, transverse speed of 10-100mm/min and pin diameter of 2-20mm. Under rotational speed of 1000-1500 RPM welding of sheets was appeared to be of good strength but it has been observed that beyond this range poor joint strength has been observed. Similarly transverse speed range out of 30-50mm/min has been selected as the final for the present case. Pin diameter from 0-6 was not able to resist the thrust force at 1000-1500 rpm and 30-50mm/min of the transverse speed and pin was broken during the welding process and similarly pin diameter of 10-20mm produced the larger welding zone which promoted the poor joining strength, so considering these issues pin diameter of 7-9mm has been selected for the present study. For preparation of design of experimentation it

was available the 3 factor with 3 level of input process parameters, so considering these input variable a orthogonal arrays of Taguchi L9 has been developed as tabulated in Table 3.

Table 3

Design of experiment based upon Taguchi L9 orthogonal arrays for FSW process.

Exp No.	Rotational Speed (rpm)	Transverse speed (mm/min)	Pin diameter (mm)
1	1000	30	7
2	1000	40	8
3	1000	50	9
4	1200	30	8
5	1200	40	9
6	1200	50	7
7	1400	30	9
8	1400	40	7
9	1400	50	8

2.6 FSW process

The conventional vertical milling machine has been used for FSW. The experimental setup configured with rotational speed of 0-2000rpm, transverse speed of 5-150mm/min. both rotational speed and transverse speed was automatically controlled to achieve the maximum accuracies during the process. The vertical milling machine was modified in such a way that table movement can be directed in both directions; i.e. from right-left or left-right and up-down or down-up. Fig. 9 shows the experimental setup and the fixture used for the FSW processes. For the final welding experimentations, two sheets of ABS-15Al with dimension of 50×30×4mm was clamped in fixture and pin of PA6-50Al was acted upon the sheets to process the FSW. The table movement was operated from left to right and pin rotation was kept in anticlockwise directions (See Fig. 3 and Fig. 9).

Following the design of experiment as per Table 3, the FSW was processed with 9 set of experiment based upon Taguchi L9 orthogonal array. The 3 level of rotational speed as; 1000, 1200 and 1400rpm, 3 level of transverse speed as; 30,40 and 50mm/min and 3 level of pin diameter 7,8 and 9 was varied to perform these set of experimentation. Fig. 10 shows the welded parts of ABS-15Al sheets prepared with semi consumable tool of PA6-50Al.

Fig. 9 Experimental setup and configuration for FSW process

Fig. 10 Welded parts as per following DOE of Table 3

2.7 Evaluation of mechanical and metallurgical properties

For evaluation of mechanical and metallurgical properties universal tensile tester, Shore D hardness and inverted microscope was used. Fig. 11 shows the pictorial view of tensile testing and shore D hardness tester used for present study. TCR was measured as mass of the pin

consumed/deposited on the welded parts. Shore D hardness (as per ASTM D2240) is one of the mechanical properties which were measured by pressing as punching knob over the specimen. Universal tensile tester as shown in Fig. 11 (as per ASTM D638) was used to calculate the peak load and peak strength of the joints as the function of tensile properties.

Fig. 11 View of tensile testing of welded parts and configuration of Shore D hardness tester

Percentage porosity at joints is the morphological property which is usually used to check the joining characteristics. In the welding practices it is usually tried to be kept as low as possible porosities of joints. The porosity can be the measure of mechanical strengths and is reversible to the mechanical properties because porous structures generally led to lesser mechanical strength. An inverted microscope with software called MIAS (Metallurgical image analysis software) was used to evaluate the morphology of the joints in form of percentage of porosity.

3. Results and Discussions

Welding process was performed by varying rotational speed, transverse speed and pin diameter. It was necessary to explain the role of these 3 parameters for variations in the tribological, mechanical and metallurgical properties so for this reason responses were optimized in the current practices.

3.1 Mechanical and metallurgical sustainability of joints

Following design of experiment as per Table 3 responses are varied accordingly as shown in Table 4. TCR was achieved maximum (21 mg/30mm welding) at experiment no. 4 and 5 and minimum (12 mg/30mm welding) was achieved at experiment no. 3. At experiment no. 5 which is the combination of rotational speed 1200rpm, transverse speed 30mm/min and 9 mm pin diameter attained maximum mechanical properties and also achieved minimum porosity. This is justified that at these rotational speed, transverse speed and pin diameter combinations the welded parts resulted in better mechanical properties, high tool consumption rate and lower porosity content. Similarly at experiment no. 3 (at 1000rpm, 50mm/min, and 9 mm pin diameter) these properties were acted opposite in nature and minimum TCR and minimum mechanical properties were observed. The welding joints were produced by following DOE as per Table 3 with 3 repetitions. The mechanical properties of joints were evaluated in 3 consecutive repetitions and average of all has been presented in Table 4. The measured value has been used for statistical analysis.

Table 4

Mechanical, tribological and morphological sustainability of welded pieces

Exp No.	TCR (mg/30mm welding)	Peak Load (Kgf)	Peak Strength(MPa)	Shore D hardness	Porosity at joints
1	14	3.41	2.84	77.0	36.48
2	15	7.58	6.35	78.5	30.65
3	12	2.51	2.09	76.5	42.21
4	21	10.35	8.43	80.0	28.06
5	21	12.41	10.34	81.5	20.08
6	20	9.08	7.57	79.5	33.98
7	14	4.99	4.06	79.0	36.65
8	16	8.15	6.79	80.0	31.41
9	15	4.34	3.53	78.5	42.58

Following the tensile properties obtained for 9 different set of experimentation a plot of stress Vs, deflection is shown in Fig. 12. As maximum tensile properties were possessed by joints at experiment no. 5, curve 5 of Fig. 12 attained a highest curve for the tensile strength. Similarly joint obtained at experiment no. 3 resulted in the lowest strength values. It was noted that at experiment no. 3 the values of strength and strain was proportionate and strength was varied according to the elongation but in the case of experiment no. 5 strength of the joints was not varied to strain and resulted in the high strength as keeping low values of elongation. Joints of Experiment no. 8 possessed maximum strain as this might have got those parametric conditions that needed for better elongation.

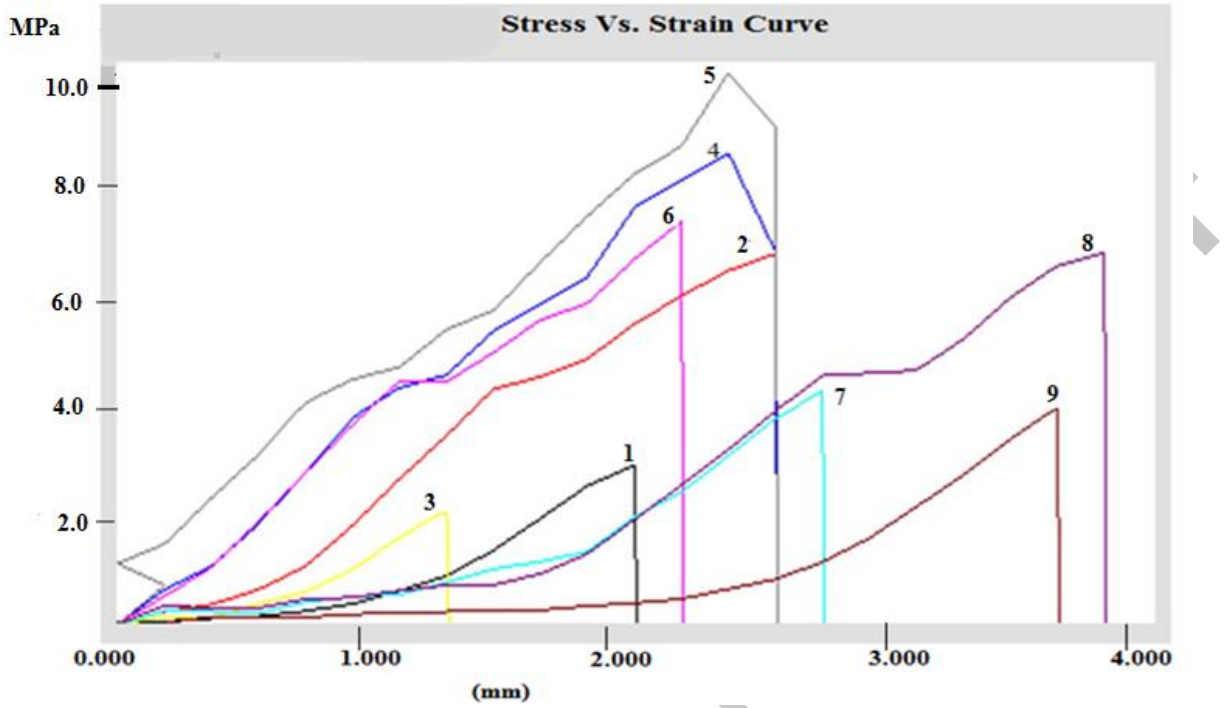

Fig. 12 Stress Vs. deflection curves of welded pieces

Stirred zone of welded pieces were examined through optical microscope by support of software tool known as "Metallurgical Image Analysis Software (MIAS)". All the welded pieces were examined at 100X of magnification level and porosity was measured at that magnification level. The welded joints processed at 1000rpm and 1400rpm have shown more porous surfaces whereas welded parts obtained at 1200rpm were appeared as less porous with better/more uniform mixing of metal powder in polymer matrix. (See Fig. 13)

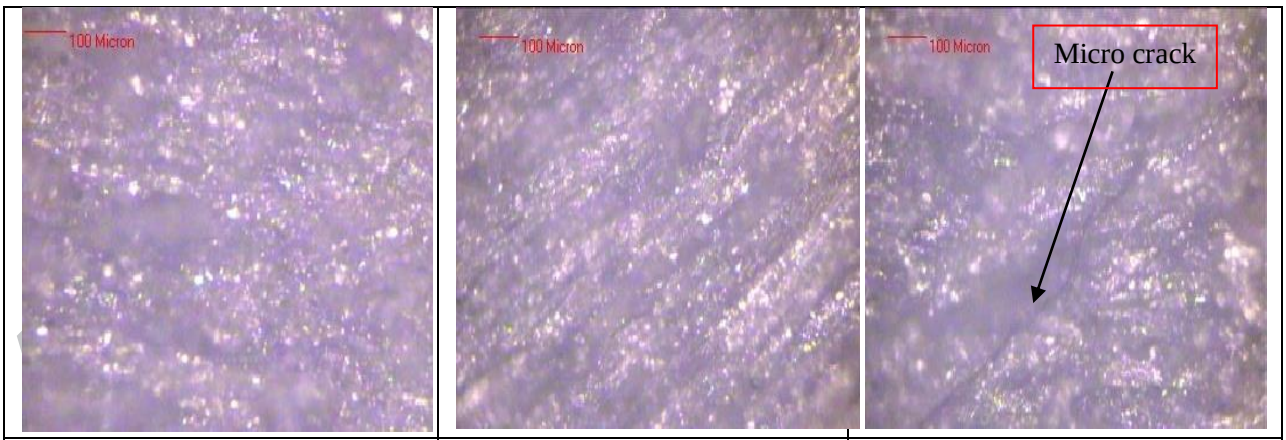

1	2	3

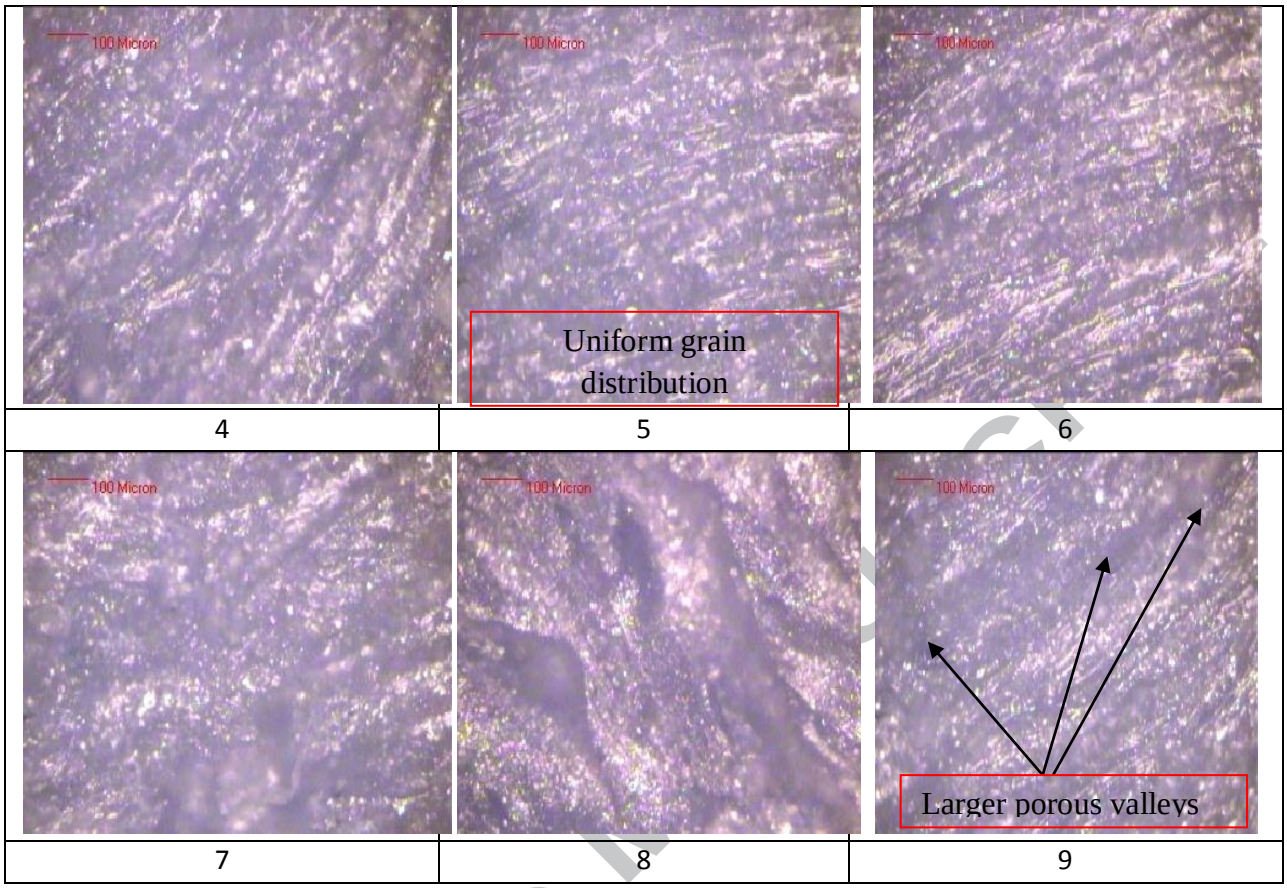

Fig. 14 Optical micrographs of welded pieces at 100X

In relation with mechanical properties to the porosity of the stirred joints, mechanical properties were varied accordingly with porosity. At experiment no. 5 where mechanical properties were resulted in maximum value, porosity came as minimum which justifies the reason for the joints strength. Improper mixing of metal powder in polymer matrix at the joint in experiment no. 9 resulted in maximum porosities and poor mechanical properties.

3.2 Optimization of process parameter

Towards optimizing input process variable for selection of best contributing process parameters, the variance over Signal to noise (SN) have been calculated. SN ratio is always desired to be maximum, conversion of material properties to SN ratio is predicted either "Smaller is better" or "Larger is better". For Mechanical properties such as; peak load, Peak strength and Shore D hardness is it required always to be maximum, so for such properties the SN ratio can be calculated as:

$$\eta = -10\, log\left[\frac{1}{n}\sum_{k=1}^{n}\frac{1}{y^2}\right]$$

For properties which desired Smaller is better, SN ratios can be calculated as;

$$\eta = -10\, log\left[\frac{1}{n}\sum_{k=1}^{n} y^2\right]$$

Where η is SN ratio, n is the no. of experiment and y is the material properties at experiment no. k. Table 5 shows the variation of SN ratios over input process variable (based upon Table 3 and 4).

Table 5

SN ratios for different properties at different processing condition

Exp No.	SN (TCR)	SN (Peak Load)	SN (Peak strength)	SN (Shore D hardness)	SN (Porosity)
1	22.92256	10.65509	9.066367	37.72981	-31.2411
2	23.52183	17.59338	16.05547	37.89739	-29.7286
3	21.58362	7.993474	6.402926	37.67323	-32.5083
4	26.44439	20.29881	18.51655	38.0618	-28.9618
5	26.44439	21.87544	20.29041	38.22315	-26.0553
6	26.0206	19.16172	17.58192	38.00734	-30.6245
7	22.92256	13.96201	12.17052	37.95254	-31.2815
8	24.0824	18.22315	16.6374	38.0618	-29.9414
9	23.52183	12.74979	10.95549	37.89739	-32.5841

Based upon Table 5, Fig. 15 shows the graphical representation for TCR, Peak load, Peak strength, Shore D hardness and porosity with respect to varying rotational speed, transverse speed and pin diameters

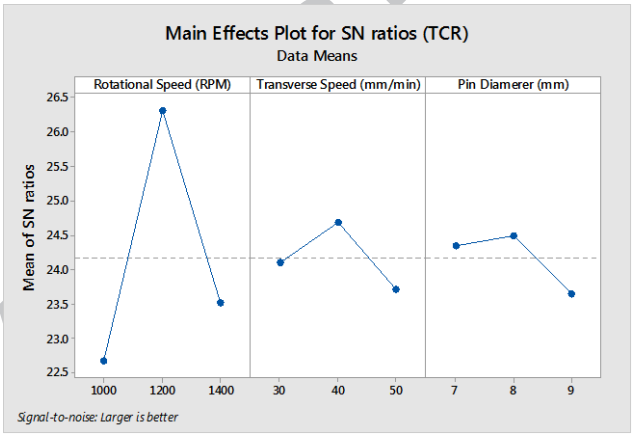

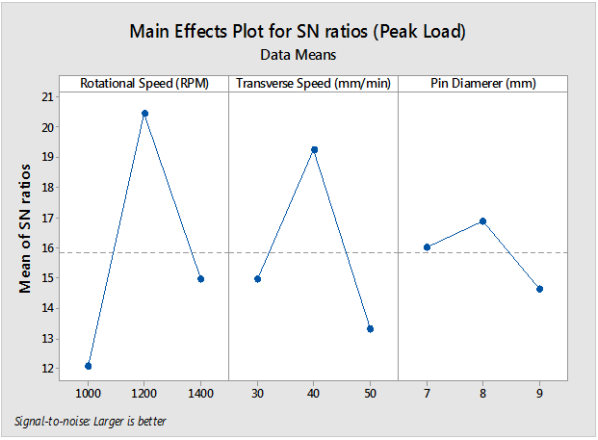

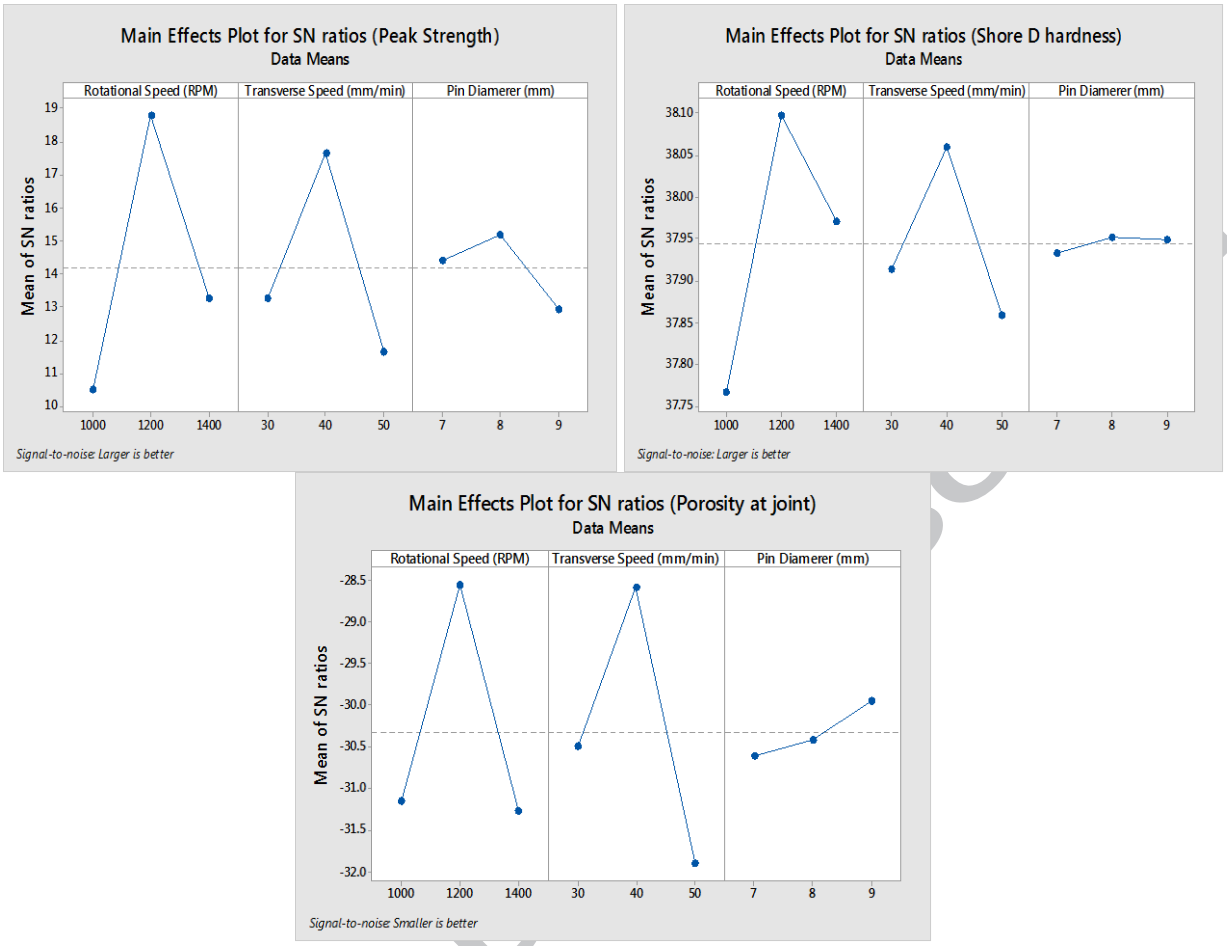

Fig. 14 Variation of SN ratios for properties over changes in input process variable

In order to optimize the process parameter for specific properties, the analysis of variance (ANOVA) table have been drawn by relating the variation of SN ratios with input parameters. Table 6 shows the ANOVA table for TCR as calculation of probability (P) and Fishers values. As P value came as <0.05 for rotational speed proves the significance of the processes (contributed 88.68%).

Table 6

Analysis of Variance for SN ratios (TCR)

Source	DF	Seq SS	Adj SS	Adj MS	F	P	%age contribution
Rotational Speed (RPM)	2	21.6573	21.6573	10.8286	213.92	0.005	88.68
Transverse Speed (mm/min)	2	1.4433	1.4433	0.7216	14.26	0.066	5.91
Pin Diameter (mm)	2	1.2176	1.2176	0.6088	12.03	0.077	4.98
Residual Error	2	0.1012	0.1012	0.0506			0.40

Total	8	24.4194					

As high TCR resulted into more strength so larger is better case was considered for calculating the SN ratios. Based upon Table 6, Table 7 shows the ranking of input process variables.

Table 7
Response Table for Signal to Noise Ratios Larger is better

Level	Rotational Speed (RPM)	Transverse Speed(mm/min)	Pin Diameter(mm)
1	22.68	24.10	24.34
2	26.30	24.68	24.50
3	23.51	23.71	23.65
Delta	3.63	0.97	0.85
Rank	1	2	3

The optimum value of TCR in this case can be predicted by using following equation:

$$\eta_{opt} = m+(m_{A2}-m) +(m_{B2}-m) +(m_{C2}-m) \quad \text{.....(ii)}$$

Where 'm' is the overall mean of SN ratio, m_{A2} is the mean of SN ratio for rotational speed at level 2, m_{B2} is the mean of SN ratio for transverse speed at level 2,and m_{C2} is the mean of SN data for pin diameter at level 2.

Now for lesser is better by type case

$$y_{opt}^2 = (1/10)^{\eta opt/10} \quad \text{.....(iii)}$$

for properties, Larger is better type case

$$y_{opt}^2 = (10)^{\eta opt\,/\,10} \quad \text{.....(iv)}$$

Calculation:

Overall mean of SN ratio (m) was taken from Minitab software.

m = 24.16 dB (See Table 5)

Now from response table of signal to noise ratio, m_{A2} = 26.30, m_{B2}=24.68, m_{C2}=24.50, (From Table 7)

Now taking equation (ii), putting the values

η_{opt}= 24.16+(26.30-24.16) +(24.68-24.16) +(24.50-24.16)

η_{opt}= 27.16

Now, from equation (iv) $y_{opt}^2 = (10)^{\eta opt\,/\,10}$

$y_{opt}^2 = (10)^{27.16/\,10}$

y_{opt} =22.80

The predicted optimum value for TCR = 22.80mg/30mm of welding

So, by applying above mentioned equation predicted value can be determined towards optimization of process parameters, for remaining output parameters (mechanical properties and

metallurgical properties). Based upon Table 5, Table 6 and Table7, the predicted and experimentally determined values of output parameters (mechanical and metallurgical properties) predicted and actual values have been shown in Table8.

Table 8

Predicted Vs actual values of output parameter at optimum predicted setting

Properties	TCR (mg/30mm welding)	Peak Load (Kgf)	Peak Strength(MPa)	Shore D hardness	Porosity at joints
Predicted Value	22.80	17.54	14.58	81.56	21.47
Actual value	21.87	17.41	14.34	81.5	21.08

3.3 Combined Optimization of process parameter

As SN ratios of all the properties have been combined by selecting SN ratios larger is better basis, 1200RPM, 40mm/min Transverse speed and 8mm pin diameter was resulted as best setting and further selected as the best set of input process parameters (See Fig. 15)

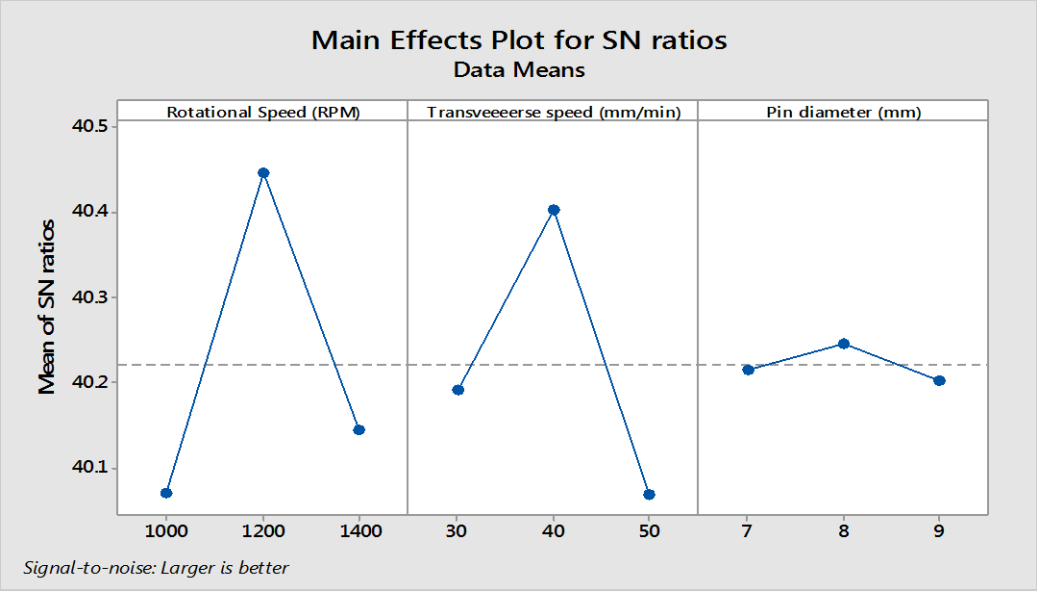

Fig. 15 Linear model graph for combined optimized set of process parameters

Since P values of RPM and transverse speed was obtained 0.008 and 0.011 which is lesser than 0.05 so combined optimized setup was predicted as significant and rpm and transverse speed was appeared as most contributing factors as 57.38% and 41.11% contributing percentage (See Table9).

Table 9
Analysis of Variance for SN ratios

Source	DF	Seq SS	Adj SS	Adj MS	F	P	%age Contributions
RPM	2	0.240230	0.240230	0.120115	125.71	0.008	57.38
Transverse speed	2	0.173525	0.173525	0.086763	90.80	0.011	41.44
Pin diameter	2	0.002934	0.002934	0.001467	1.54	0.394	0.70
Residual Error	2	0.001911	0.001911	0.000956			0.68
Total	8	0.418600					

4. Conclusions

In this manuscript a frame work for measuring rheological, mechanical and thermal properties of functional prototypes (joint produced with dissimilar thermoplastics) has been outlined. It should be noted that in this study the FSW of ABS-15Al sheets (as work piece) with three different diameters of tool material PA6-50Al (as tool) has been reported. For making the joint the same tool has been used for three times (as per DOE suggested, see Table3). Following conclusions have been drawn from the present study:

- Welding of virgin ABS sheets with virgin PA6 pin parts was unsuccessful due to the dissimilarities in their melt flow properties. Reinforcement of 15% Al content to ABS and 50% Al content to PA6 matrix resulted in the similar MFI range of 11.57g/10min and 11.97g/10min respectively.
- Reinforcement of 15% Al content in ABS led to increase in the melting point from 201.22^{o}C to 218.11^{o}C and reinforcement of 50% Al content to PA6 led to modification in the melting point from 218.35^{o}C to 218.27^{o}C. The reinforcement caused the material to be thermally compatible to each other used for FSW application.
- As predicted from the combined optimization, 1200rpm, 40mm/min transverse speed and 8 mm pin diameter may be selected combination of input variables so as to maximize the strength, hardness, load and tool consumption rate and to minimize porosity on the stirred zone.

Acknowledgement
The authors are highly thankful to Board of research in nuclear science (BRNS) No: 34/14/10/2016-BRNS/34036 for providing financial assistance to carry out the research work.

References

1] Singh R, Kumar R, Feo L, Fraternali F. Friction welding of dissimilar plastic/polymer materials with metal powder reinforcement for engineering applications. Composite Part B Engineering, 2016;101:77–86. doi:https://doi.org/10.1016/j.compositesb.2016.06.082.

[2] Kumar R, Singh R, Ahuja IPS. A framework for welding of dissimilar polymers by using metallic fillers, IJMER 2017;8:101–5.

[3] Singh R, Kumar R, Kumar S. Polymer Waste as Fused Deposition Modeling Feed Stock Filament for Industrial Applications. Ref Modul Mater Sci Mater Eng 2017:1–12. doi:10.1016/B978-0-12-803581-8.04153-9.

[4] Singh R, Kumar R, Hashmi MSJ. Friction Welding of Dissimilar Plastic-Based Material by Metal Powder Reinforcement. vol. 13. Elsevier Ltd.; 2017. doi:http://dx.doi.org/10.1016/B978-0-12-803581-8.04159-X.

[5] Hu X, Chen Y, Liang H, Xiao C. Preparation of pressure responsive hollow fiber membrane by melt-spinning of polyurethane-poly(vinylidene fluoride)-Poly(ethylene glycol) blends. Mater Manuf Process 2010;25:1018–20. doi:10.1080/10426910903367378.

[6] Huang ZX, Meng C, Zhang G, Qu JP. Manufacturing polymer/clay nanocomposites through elongational flow technique. Mater Manuf Process 2017;32:1409–15. doi:10.1080/10426914.2017.1339316.

[7] Olakanmi EO, Thompson OM, Vunain E, Doyoyo M, Meijboom R. Effects of Daniella oliveri Wood Flour Characteristics on the Processing and Functional Properties of Wood Polymer Composites. Mater Manuf Process 2016;31:1073–84. doi:10.1080/10426914.2015.1037895.

[8] Ray S, Easteal AJ. Advances in polymer-filler composites: Macro to nano. Mater Manuf Process 2007;22:741–9. doi:10.1080/10426910701385366.

[9] Singh K, Nanda T, Mehta R. Processing of polyethylene terephthalate fiber reinforcement to improve compatibility with constituents of GFRP nanocomposites. Mater Manuf Process 2017;6914:1–9. doi:10.1080/10426914.2017.1291955.

[10] Alagar M, Thanikai Velan T V., Ashok Kumar A, Mohan V. Synthesis and characterization of high performance polymeric hybrid siliconized epoxy composites for aerospace applications. Mater Manuf Process 1999;14:67–83. doi:10.1080/10426919908914805.

[11] Wan Y, Tang B, Liu C, Gao Y, Jiang S. Effect of Dy and Nd on ZK10 alloy processed by hot extrusion. Mater Manuf Process 2017;32:1360–2. doi:10.1080/10426914.2017.1303160.

[12] Venkatesh C, Venkatesan R. Optimization of process parameters of hot extrusion of SiC/Al 6061 composite using Taguchi's technique and upper bound technique. Mater Manuf Process 2015;30:85–92. doi:10.1080/10426914.2014.962658.

[13] Mewis J, Jansseune T. Rheology and morphology of concentrated immiscible polymer blends. Korea-Australia Rheol 2001;13:189–96.

[14] Chaitanya S, Singh I. Processing of PLA/sisal fiber biocomposites using direct- and extrusion-injection molding. Mater Manuf Process 2017;32:468–74. doi:10.1080/10426914.2016.1198034.

[15] Azarsa E, Mostafapour A. On the feasibility of producing polymer-metal composites via novel variant of friction stir processing. J Manuf Process 2013;15:682–8. doi:10.1016/j.jmapro.2013.08.007.

[16] Squeo EA, Bruno G, Guglielmotti A, Quadrini F. Friction stir welding of polyethylene sheets. Frict Stir Weld Polyethyl Sheets 2009:241–146.

[17] From D. Downloaded From: http://proceedings.asmedigitalcollection.asme.org/ on 01/31/2016 Terms of Use: http://www.asme.org/about-asme/terms-of-use 2016:1–4.

[18] Oliveira PHF, Amancio-filho ST, Santos JF, Jr EH. Preliminary study on the feasibility of friction spot welding in PMMA. Mater Lett 2010;64:2098–101. doi:10.1016/j.matlet.2010.06.050.

[19] Simoes F, Rodrigues DM. Material flow and thermo-mechanical conditions during Friction Stir Welding of polymers: Literature review, experimental results and empirical analysis. Mater Des 2014;59:344–51. doi:10.1016/j.matdes.2013.12.038.

[20] Abibe AB, Sônego M, dos Santos JF, Canto LB, Amancio-Filho ST. On the feasibility of a friction-based staking joining method for polymer-metal hybrid structures. Mater Des 2016;92:632–42. doi:10.1016/j.matdes.2015.12.087.

[21] Goncalves J., Dos Santos J. F., Canto L. B., & Amancio-Filho S. T. Friction spot welding of carbon fiber-reinforced polyamide 66 laminate. *Materials Letters 2015*: *159*; 506-509.

[22] Buffa G, Baffari D, Campanella D, Fratini L. An Innovative Friction Stir Welding Based Technique to Produce Dissimilar Light Alloys to Thermoplastic Matrix Composite Joints. Procedia Manuf 2016;5:319–31. doi:10.1016/j.promfg.2016.08.028.

[23] Paoletti A, Lambiase F, Di Ilio A. Optimization of Friction Stir Welding of Thermoplastics. Procedia CIRP 2015;33:563–8. doi:10.1016/j.procir.2015.06.078.

[24] Vijendra B, Sharma A. Induction heated tool assisted friction-stir welding (i-FSW): A novel hybrid process for joining of thermoplastics. J Manuf Process 2015. doi:10.1016/j.jmapro.2015.07.005.

[25] Rezaee Hajideh M, Farahani M, Alavi SAD, Molla Ramezani N. Investigation on the effects of tool geometry on the microstructure and the mechanical properties of dissimilar friction stir welded polyethylene and polypropylene sheets. J Manuf Process 2017;26:269–79. doi:10.1016/j.jmapro.2017.02.018.

[26] Hamdollahzadeh A, Bahrami M, Nikoo MF, Yusefi A, Givi MKB, Parvin N. Microstructure evolutions and mechanical properties of nano-SiC-fortified AA7075 friction stir weldment: The role of second pass processing. J Manuf Process 2015. doi:10.1016/j.jmapro.2015.06.017.

[27] Gamit D, Mishra RR, Sharma AK. Joining of mild steel pipes using microwave hybrid heating at 2.45 GHz and joint characterization. J Manuf Process 2017;27:158–68. doi:10.1016/j.jmapro.2017.04.028.

[28] Eslami S, Ramos T, Tavares PJ, Moreira PMGP. Shoulder design developments for FSW lap joints of dissimilar polymers. J Manuf Process 2015;20:15–23. doi:10.1016/j.jmapro.2015.09.013.

[29] Lambiase F, Paoletti A, Grossi V, Ilio A Di. Friction assisted joining of aluminum and PVC sheets. J Manuf Process 2017;29:221–31. doi:10.1016/j.jmapro.2017.07.026.

[30] Azarsa E, Mostafapour A. Experimental investigation on flexural behavior of friction stir welded high density polyethylene sheets. J Manuf Process 2014;16:149–55. doi:10.1016/j.jmapro.2013.12.003.

[31] Kumar R, Chattopadhyaya S, Dixit AR, Bora B, Zelenak M, Foldyna J, Hloch S., Hlavacek P, Scucka J, Klich J. and Sitek L. Surface integrity analysis of abrasive water jet-cut surfaces of friction stir welded joints. The International Journal of Advanced Manufacturing Technology 2017; 88(5-8): 1687-1701.

[32] Kumar R, Chattopadhyaya S, Ghosh A, Krolczyk GM., Vilaca P, Kumar R, Srivastava M, Shariq M, and Triphathi R. Characterization of friction surfaced coatings of AISI 316 tool over high-speed-steel substrate. Transactions of FAMENA 2017: 41 (2); 61-76.

[33] Kumar R, Bora B, Chattopadhyaya S, Krolczyk G, Hloch S. Development of mathematical Model based on Mechanical and Thermal Properties for Friction Stir Welded Joint. Int. J. of Materials and Product Technology, Inderscience J. April, 2017.

Manuscript Highlights:

- Solution for compatibility issues between two dissimilar thermoplastic materials.
- MFI of ABS and PA 6 was modeled by reinforcement of Al metal powder.
- Reinforcement of 15% Al in ABS and 50% Al in PA6 resulted in thermally compatibility.
- Suggested settings are 1200rpm, 40mm/min transverse speed and 8 mm pin diameter.